
Assessment of Remotely Sensed Indices to Estimate Soil Salinity

Naser Ahmadi Sani ^{a*}, Mohammad khanyaghma ^b

^a *Assist. Prof., Faculty of Agriculture and Natural Resources, Mahabad Branch, Islamic Azad University, Mahabad, Iran*
^b *MSc of Agroecology, Mahabad Branch, Islamic Azad University, Mahabad, Iran*

Received 17 March 2018; revised 4 October 2018; accepted 5 October 2018

Abstract

Soil Salinization is one of the oldest environmental problems and one of the main paths to desertification. Access to information in the shortest time and at low cost is the major factor influencing decision making. The satellite imagery provides information data on salinity and also offers large amount of data that can be analyzed and processed to understand several indices based on the type of the sensor used. In this research, the capability of different indices derived from IRS-P6 data was evaluated to identify saline soils in Mahabad County. The quality of the satellite images was first evaluated and no noticeable radiometric and geometric distortion was detected. The Ortho-rectification of the image was performed using the satellite ephemeris data, digital elevation model, and ground control points. The RMS error was less than a pixel. In this study, the correlation between the bands and used indices, including Salinity1, Salinity2, Salinity3, PCA1 (B2, B3), PCA1 (B4, B5), PCA1 (B1, B2, B3, B4, B5), Fusion (Pan and B2), Fusion (Pan and B3) and Fusion (Pan and B4) with EC were investigated. The highest correlation was related to the Fusion (Pan and B2) with a coefficient 0.76 and the lowest correlation was related to B4 with a coefficient 0.2. The results showed that the indices have a high ability for modeling, mapping and estimating the soil salinity.

Keywords: Indices, IRS-P6, Remote sensing, Soil Salinity

1. Introduction

Salinization is one of the most common land degradation processes in arid and semi-arid areas. It is one of the oldest environmental problems and paths to desertification (Morshed et al., 2016).

* Corresponding author. Tel: +98-9142960454.

E-mail address: n.ahmadisani@gmail.com.

Salinity usually refers to a significant concentration of mineral salts in soil or water because of the hydrological processes (Schofield et al. 2001). There are two main types of salinization: primary and secondary. Primary salinization occurs through the natural processes. Secondary salinization occurs due to poor management practices (Mashimbye, 2013). The effects of salinization can be observed in numerous vital ecological and non-ecological soil functions (Daliakopoulos et al., 2016). Soil salinity can reduce the productivity of affected lands, posing degradation, and threats to sustainable development (Yu et al., 2018).

Planning for each type of activity requires correct and timely information. The required data and information can be obtained in different ways like field inventory and remote sensing. By using field method one can acquire data with the desired spatial and descriptive accuracy, but generally it is time-consuming and costly. In contrast, by using remote sensing technology in several fields, the required data can be quick and efficient (Makhdoum et al., 2009; Ahmadi Sani et al., 2011).

By the launch of Landsat in 1972, remote sensing technology opened a new horizon into the planning and management of different resources. This issue supplies a new method for surveying and estimating different parameters (Alavipanah and Ladani, 2010). In this regard, the role of RS is directly and indirectly proved by providing new chances for using different satellite images and various methods of classifying and mapping (Ahmadi Sani et al., 2011). Remote sensing data are considered to be a convenient source to extract several indices in either simple or complicated band ratio combinations. Satellite images offer a large amount of data that could be analyzed, processed and stored for better understanding of several indices based on the type of the used sensors (Elhag and Bahrawi, 2017).

With saline and sodic soils covering of 93232 million hectares globally, and one of the major soil degradation threats worldwide, with mismanaged irrigation affecting 34.19 million hectares or over 10% of the total irrigated lands, soil salinization is a widespread phenomenon. The excessive accumulation of soluble salts in the soil surface influences soil properties, which decreases soil productivity, limits the growth of crops, and constraints agricultural productivity. Excessive concentration of salts in soil may lead to the abandonment of agricultural land. Globally, the cost of irrigation-induced salinity is equal to an estimated US\$11 billions per year (Morshed et al., 2016).

Various remote sensing data are being used for identifying and monitoring salt-affected areas such as aerial photographs, infrared thermography, visible and infrared multispectral, and microwave images (Metternicht and Zinck 2003). Regarding the importance of indices in soil salinity mapping, various researchers have been using different indices (Fernandez-Buses et al., 2006; Morshed et al., 2016). They have introduced different and sometimes similar indices as the best indices for soil salinity evaluation. But results have shown that one can use the indices instead of single and original bands for more exact mapping and information extraction of soils saline. Therefore, in this study the possibility of using some indices of earlier studies was evaluated for soil salinity mapping using IRS-P6 data.

2. Materials and Methods

2.1. The Study Area

The study area is located in West Azerbaijan Province, north of Mahabad County, with an area of about 33,000 hectares. The climate of the area is cold and humid and the average annual precipitation is about 356 mm. Most of the area is allocated to agricultural lands. The major crops in the region are cereals, sugar beet, alfalfa, cucurbits, legumes, apple and stone fruit orchards. Ranges and residential areas also occupy a small percentage of the area.

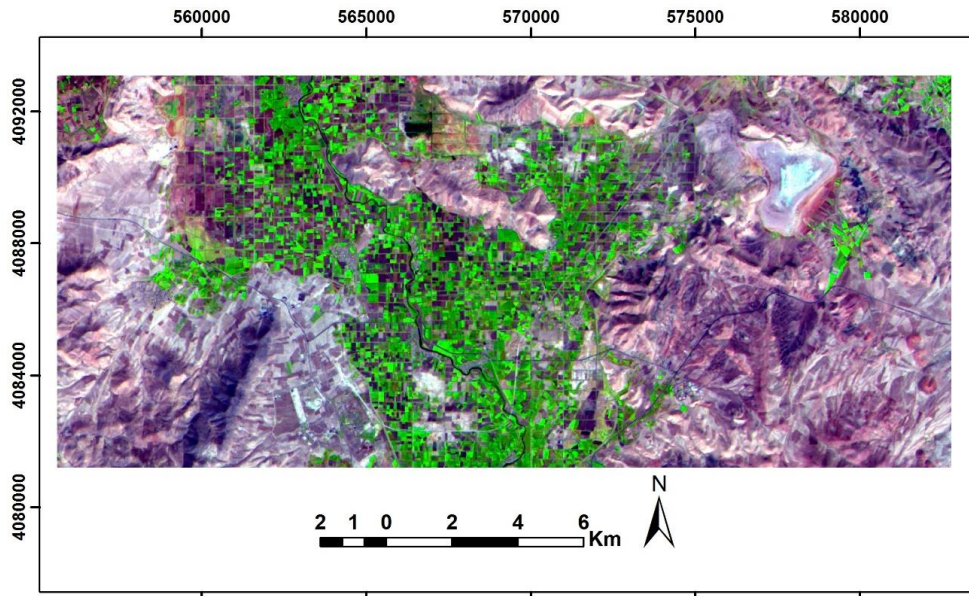


Figure 1. A view of the study area (RGB₅₄₃)

2.2. Methodology

This paper has made an attempt to measure the soil salinity from remote sensing indices analysis. To predict soil salinity, an integrated approach of salinity indices and field data was used. The correlations between different indices and field data of soil salinity were calculated to find out the highly correlated indices. The stepwise regression analysis was done to determine the combination of indices and bands that showed the best correlation with the field EC values. The research method is shown in Figure 2.

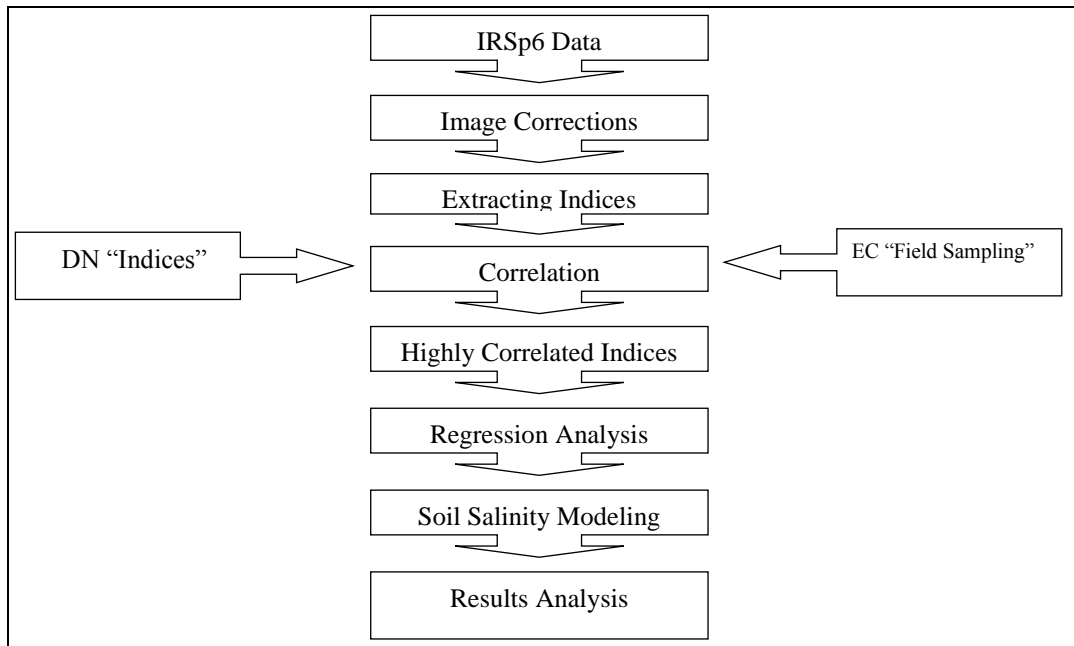


Figure 2. Flowchart of research methodology

2.2.1. Satellite Data

In this research, IRS-P6 satellite data, including panchromatic band and the multi-spectral bands were used. The data were gathered in summer of 2011 because the best images to study the soil salinity are the images that have the least plant cover at the time of imaging the soil.

2.2.2. Data Corrections

All raw satellite data have geometric errors. Radiometric errors are visible if present. In this study, there was no significant radiometric error, and geometric corrections were made in two ways: 1. Images to map using the map of rivers and roads and by the method of Ortho-rectification for the correction of panchromatic band. 2. Using images to image for correction of spectral bands using the corrected band as the basis.

2.2.3. Indices and Synthetic Bands

Many researchers have used various indices to prepare soil salinity maps (Daliakopoulos et al., 2016; Elhag and Bahrawi, 2017; Medjani et al., 2017; Morshed et al., 2016; Fourati et al., 2015; Daempanah et al., 2011; Dashtakian et al., 2008), so some indices are known and can be used in soil salinity mapping. Indices, in addition to increasing the clarity and improving categorization of phenomena, reduce the negative effects of inappropriate factors and the effects of other land covers.

In this research, by applying the methods of Ratioing, Principal Components Analysis and also Fusion in order to import spatial precision of panchromatic band into multi-spectral bands to better fit the true values of salinity and digital values of images in different locations. Therefore, several indices and synthetic bands were developed and used in the analysis.

2.2.4. Soil Sampling

In this research, systematic sampling was used. A regular grid, 1000×1000 meter, was deployed by GPS in the area and Surface soil samples were taken. Sampling was done in September to adapt the time between imagery and sampling. The vegetation areas, orchards, inaccessible areas and mountains were eliminated. Finally, 147 samples were taken and the electrical conductivity of each sample in the soil laboratory was extracted. By entering the salinity data (EC) into the grid map table, a point salinity map was prepared.

2.2.5. Extract of the Corresponding Values

After bands correction and preparing of different indices, the vector map of the sampling grid was placed on bands and indices. The pixel digital number which was placed at each sampling point was recorded as the digital number of that point in the images in the ArcGIS environment. This work was carried out for all sampled points and for all the bands in the study area. Finally, the values for each band (main and synthetic), along with the amount of salinity, were entered into the SPSS software for last analysis.

2.2.6. Statistical Analysis

At first descriptive statistics of EC were extracted, including average, mode, mean, and standard deviation, standard error, maximum and minimum. The histogram was then plotted and the data were normalized by log-transforming, which was tested by Kolmogorov-Smirnov test. Finally, correlation, regression, and variance analysis were investigated to verify the significance of the data. Also, the stepwise regression analysis was performed and a salinity model was developed.

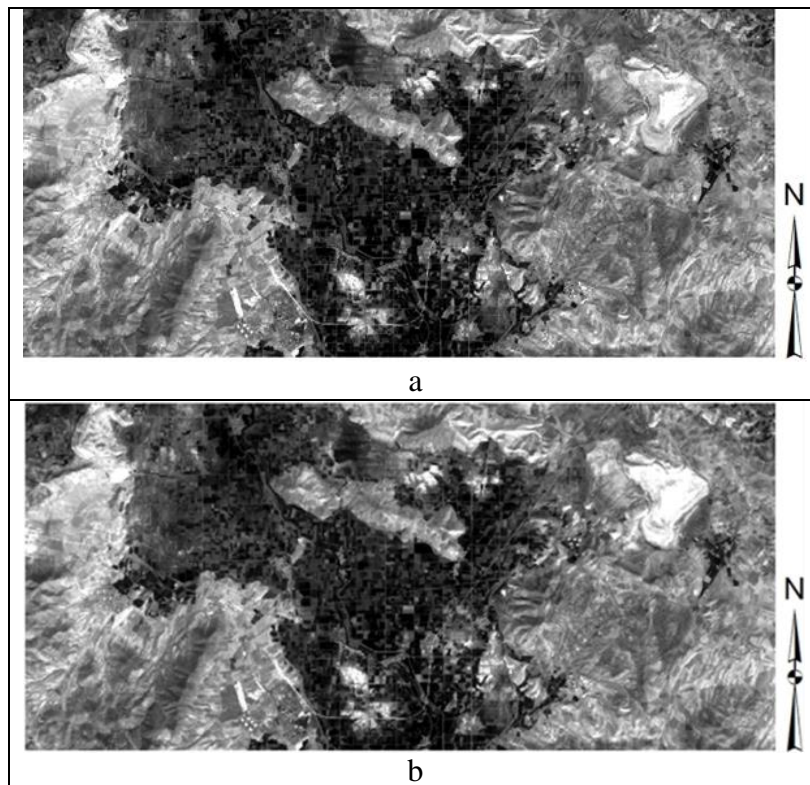
Table 1. Used indices and formula

| Indices | Formula |
|------------------|-------------------------------------|
| Salinity1 | $(B2 + B3)^{0.5}$ |
| Salinity2 | $(B2^2+B3^2+B4^2)^{0.5}$ |
| Salinity3 | $(B2^2+B3^2)^{0.5}$ |
| PCA1 (2,3) | The first component of PCA on B2,3 |
| PCA1 (4,5) | The first component of PCA on B4, 5 |
| PCA1 (1,2,3,4,5) | The first component of PCA on B1-5 |
| Fusion (Pan, B2) | Fusion of B2 with Pan |
| Fusion (Pan, B3) | Fusion of B3 with Pan |
| Fusion (Pan, B4) | Fusion of B4 with Pan |

3. Results and Discussion

Regarding investigations on different bands of IRS-P6 images, no considerable radiometric error was observed. Geometrical correction of images was done using an Ortho-rectification method with RMSE of less than one pixel. The indices were prepared using Fusion, PCA and Salinity indices (Figures 3-5).

Fusion can in general be done at different levels namely pixel level, feature level, object level and decision levels (Subramanian et al., 2006). There are many image fusion methods that can be used to produce high resolution multispectral images from a high resolution pan image and low resolution multispectral images, including component substitution numerical methods, statistical image fusion, multi-resolution approaches and hybrid techniques. Mathematical combinations of different images are among the simplest and earliest methods used in remote sensing (Pohl and Van Genderen, 2017). In this study, numerical method (sum) has been used for fusion of panchromatic and multispectral bands (Figure 3).



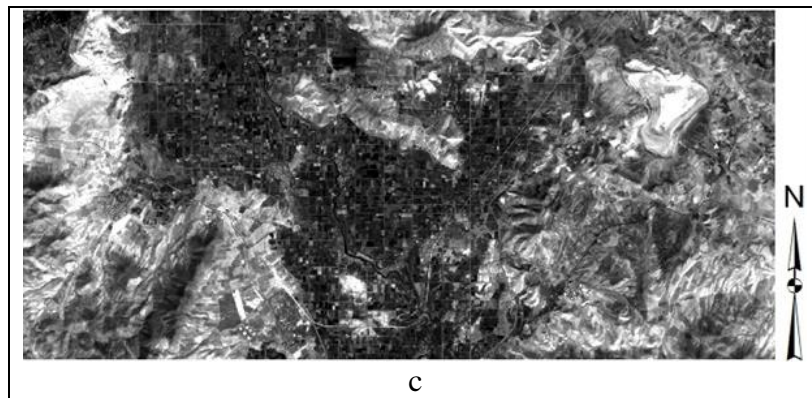
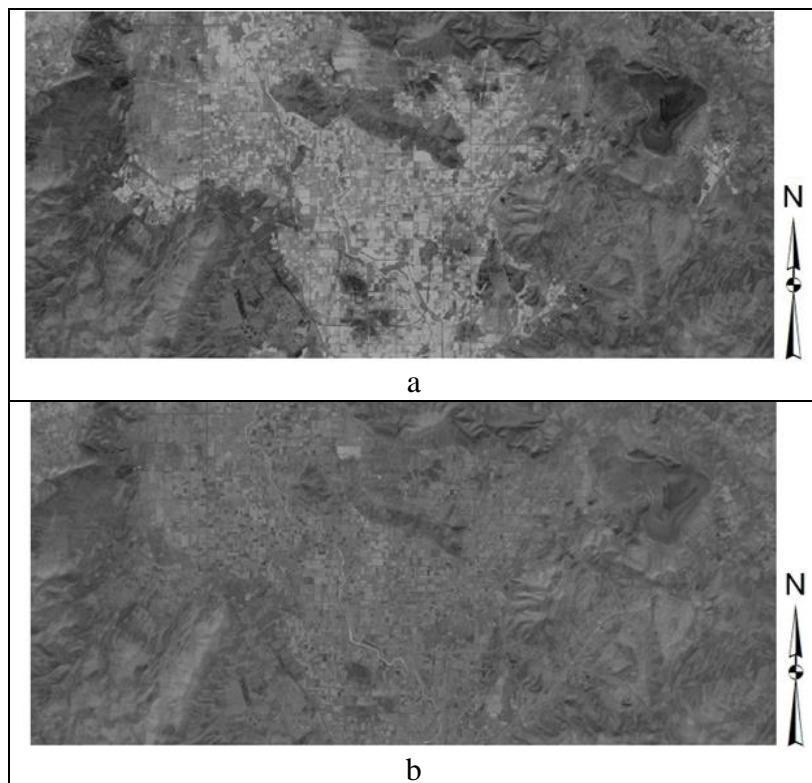


Figure 3. Fusion indices; a (B2 & Pan), b (B3 & Pan), c (B4 & Pan)

The principal component analysis technique was applied to the 4 temporal data sets of SWIR, NIR, Red and Green bands, to de-correlate possible redundant information into some PCs (Pattanaik et al., 2008). It was found that the first PCs concentrated on most of the information of necessity showing highest variance percentage among all other PCs (Figure 4).



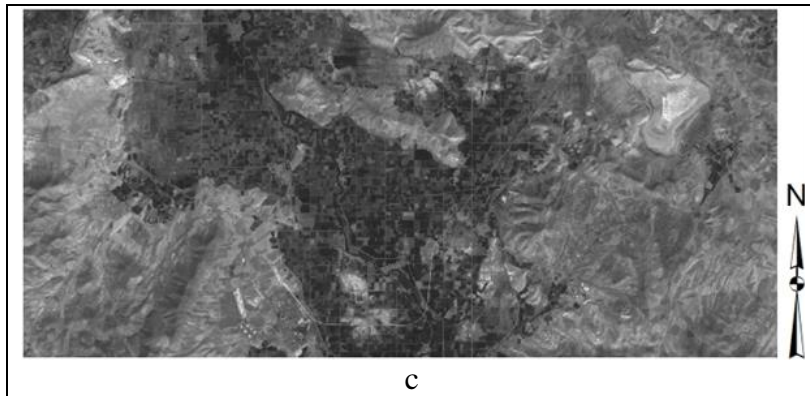
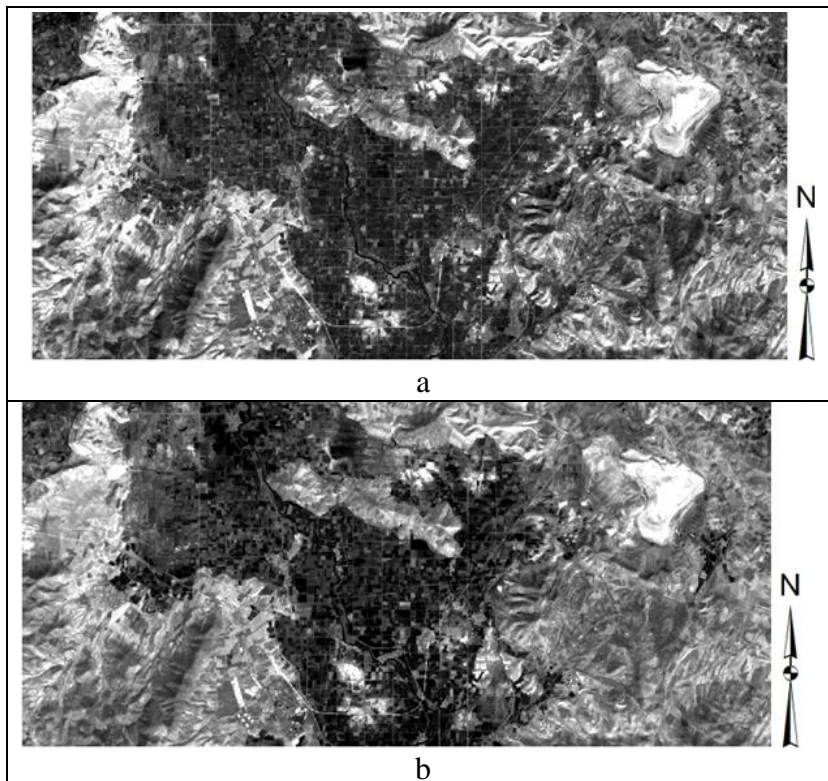


Figure 4. PCA indices; a (PC1B2 & B3), b (PC1B4 & B5), c (PC1B1 & B5)

Soil salinity indices are principally adjusted to detect salt mineral in soils based on the different responses of salty soils to various spectral bands (Elhag and bahrawi, 2017). Among the three computed spectral salinity indices (Figure 5), S11 offers the highest correlation coefficient (Fourati et al., 2015; Yu et al., 2018).



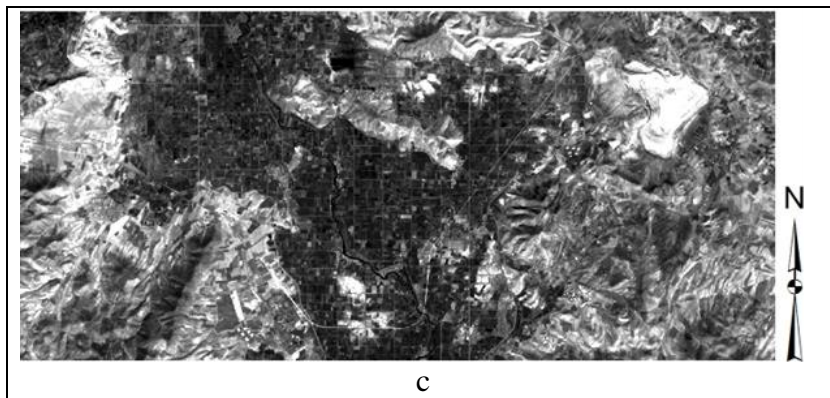


Figure 5. Salinity indices; a (Salinity1), b (Salinity2), c (Salinity3)

As the figures show visually, the fusion index of (Pan, B2) has shown the salinity changes better than other indices. The descriptive statistics calculation of EC showed that the average amount of salinity was 54.7 ds/m and data variance, standard deviation and median were 54, 58 and 87 respectively. The lowest amount of EC was 0.31 and the highest was 26.19 and the range of electrical conduction was 25.88.

Comparison of correlation coefficient among main bands and indices with EC showed that B2 (0.73) and (Pan +B2) fusion index (0.76) had the highest correlations. Also, in this research, B4 (0.2) had a very poor correlation (Fourati et al., 2015). Regarding the correlation between bands and indices, highest correlation (0.994) belonged to B3 and salinity1 index (Fourati et al., 2015; Bouaziz et al., 2011) and indices PCA23, PCA45 had negative correlation. The stepwise regression analysis showed a relatively good salinity model in comparison with the earlier research studies (Abdinam, 2004) including only one index (fusion of Pan and B2) with a correlation coefficient equal to 0.628 and Radj equal to 0.39. The regression equation combining remote sensing indices which is shown in Equation 1.

$$\text{Salinity} = 0.046 * \text{Fusion} (\text{B2}, \text{Pan}) - 0.858 \quad (1)$$

Table 2. Some Correlation Coefficients

| Bands and Indices | EC | Pan | B2 | B4 | Salinity1 | Salinity3 | PCA1 (1-5) | Fus (Pan,2) |
|---------------------|------|------|------|------|-----------|-----------|------------|-------------|
| Pan | 0.7 | 1 | | | | | | |
| B2 | 0.73 | 0.88 | 1 | | | | | |
| B4 | 0.2 | 0.11 | 0.26 | 1 | | | | |
| Salinity1 | 0.71 | 0.9 | 0.99 | 0.19 | 1 | | | |
| Salinity3 | 0.72 | 0.9 | 0.99 | 0.21 | 0.99 | 1 | | |
| PCA1 (1-5) | 0.72 | 0.93 | 0.98 | 0.26 | 0.99 | 0.99 | 1 | |
| Fus (Pan, 2) | 0.76 | 0.97 | 0.97 | 0.21 | 0.97 | 0.97 | 0.99 | 1 |
| Fus (Pan, 4) | 0.66 | 0.78 | 0.71 | 0.68 | 0.77 | 0.78 | 0.83 | 0.82 |

The results showed that Pan and B2 bands had the highest correlation with electrical conductivity, so it is reasonable that the fusion index (Pan, B2) has the highest correlation with salinity values. The correlation of EC with the indices used in this research was high except for Fusion (Pan, B4), PCA1 (B4, B5) and salinity2 indices so it could be related to the use of B4 in preparation of these indices; because as the salinity increases, the spectral value of the near-infrared band decreases. The results of regression analysis showed that among all the bands and indices, only Fusion (Pan, B2) index has a significant correlation with salinity changes. The resulting amounts R^2 and Radj do not have any significant difference with the results of other research studies (Fourati et al., 2015; Bouaziz et al., 2011; Tajgardan et al., 2009; Dadresi and Pakparvar, 2007). In the earlier studies, different researchers recommended different bands and indices for salinity evaluation. Therefore, even if one index had no importance in an area, it is possible to be suitable for other areas. It means that in the areas with different salinity, climate, geographical and geological conditions, different indices can describe salinity changes. The best correlation coefficient of satellite data with electrical conductivity changes in this study compared with earlier studies (Abdinam, 2004; Dadresi and Pakparvar, 2007; Bouaziz et al., 2011), showed potential of IRS-P6 data for soil surface salinity mapping. Also, in confirmation of earlier studies, the use of correlation and regression between satellite data with salinity values facilitate soil mapping with less time and cost required (Alavipanah and Ladani, 2010; Meng et al., 2016).

As Table 3 shows, the use of regression and ETM+ data has been more common, so the investigation of the IRS-P6 data capability requires more studies. Moreover, the best bands and indices included SWIR band, PCA indices and salinity indices in different studies (Table 3). There are differences in some studies (Tajgardan et al., 2009; Bouaziz et al., 2011; Meng et al., 2016) for example the near-infrared band is the best band, which can be due to the use of different data and conditions of the studied area, including vegetation type and density. However, this integrated approach has the potential for detecting soil salinity over local scale efficiently and economically (Morshed et al., 2016) and provide tools for soil salinity monitoring and the sustainable utilization of land resources (Yu et al., 2018).

Table 3. Comparison of past studies

| Study | Indices | Methods | Data | The Best |
|-----------------------------|---------------------------|----------------|---------|----------------|
| Abdinam, 2004 | Color Composite (FCC742) | Regression | ETM+ | B7 |
| Dadresi and Pakparvar, 2007 | Different Ratioings + PCA | Classification | TM | PCA 234-FCC521 |
| Dashtakian et al., 2008 | BI-SI-NDSI-YSI | Regression | ETM+ | SI |
| Tajgardan et al., 2009 | SI1-3, BI-MSI-PCA-Fusion | Regression | ETM+ | B4-FusB4 |
| Daempanah et al., 2011 | PCA SI1-SI2- BI-NDSI | Regression | IRS-P6 | SI1 |
| Bouaziz et al., 2011 | NDVI- SAVI- SI- SI1- SI2 | Regression | MODIS | SI2- SWIR- NIR |
| Fourati et al., 2015 | BI-SI-SI1-SI2-SI3 | Regression | OLI | SI- SI3 |
| Meng et al., 2016 | NDSI- BI- SI- COSRI | Regression | ETM+OLI | NDSI- SWIR-NIR |
| Morshed et al., 2016 | BI-SI1-SI2-SI3-NDVI-EVI | Regression | ETM+ | NIR-SWIR-SI2 |
| Medjani et al., 2017 | BI-NDVI-PCI | Classification | ETM+ | BI-PCA |

4. Conclusion

This paper has presented the potential of integrating IRS-P6 data analysis and field survey data to assess and monitor soil salinity over a local scale. The correlations between the field EC and salinity indices is relatively good and about 40%, variation was observed between the field data and predicted EC by the indices analysis. The results compared to other studies showed that depending on the land physiographic, vegetation, climate and land use, the degree of salinity and geology, different sensors, bands, and indices can be used for soil salinity estimation. Therefore, in this study although Pan and B2 bands are highly correlated with changes in the electrical conductivity of soil, fusion index (Pan, B2) gave better results. The results of the indices showed that they are important for improving the accuracy of the soil salinity map. The Use of the hottest month images of the year, due to the maximum evaporation and salt accumulation in the soil surface can be more effective for estimation of soil salinity. The study showed the high-capability of IRS-P6 data to produce a soil salinity map. Also, in addition to simplicity and high precision using correlation and regression methods between satellite data (DN) and soil salinity (EC) facilitates mapping of soil salinity with more efficiency. It is suggested that in the future, data with a wider spectral range, SWIR and TIR bands, along with other indices be evaluated for preparing salinity maps.

References

- Abdinam, A. (2004). The mapping of soil salinity using the correlation between satellite data and salinity values in Qazvin plain. *PAJOUHESH-VA-SAZANDEGI*, 17(3), 33-38.
- Ahmadi-Sani, N., Babaei-Kafaky, S., & Mataji, A. (2011, May). Application of GIS and remote sensing in ecological capability assessment studies. 18th Geomatics Conference, National Cartographic Center, Tehran.
- Alavipanah, S. K., & Ladani, M. (2010). *Remote Sensing and Geographic Information System*. Tehran University Press.
- Bouaziz, M., Matschullat, J., & Gloaguen, R. (2011). Improved remote sensing detection of soil salinity from a semi-arid climate in Northeast Brazil. *Comptes Rendus Geoscience*, 343(11-12), 795-803.
- Dadresi-Sabzevari, A., & Pakparvar, M. (2007). The trend of desertification using remote and near sensing in Sabzevar. *Iranian Journal of range and desert Researches*, 14(1), 33-52.
- Daempanah, R., Haghnia, G., Alizadeh, A., & Karimi, A. (2011). Mapping of soil salinity and alkalinity using remote sensing and geostatistical methods in Mahvelat city. *Journal of Water and Soil*, 25(3), 498-508.
- Daliakopoulos, I. N., Tsanis, I. K., Koutroulis, A., Kourgialas, N. N., Varouchakis, A. E., Karatzas, G. P., & Ritsema, C. J. (2016). The threat of soil salinity: A European scale review. *Science of the Total Environment*, 573, 727-739.
- Dashtkian, K., Pakparvar, M., & Abdullahi, J. (2008). Investigation of soil salinity mapping methods using Landsat satellite data in Marvast area. *Iranian Journal of range and desert Researches*, 15(2), 139-157.

- Elhag, M., & Bahrawi, J. A. (2017). Soil salinity mapping and hydrological drought indices assessment in arid environments based on remote sensing techniques. *Geoscientific Instrumentation, Methods and Data Systems*, 6(1), 149-158.
- Fernandez-Buses, N., Siebe, C., Cram, S., & Palaci, J. L. (2006). Mapping soil salinity using a combined spectral response index for bare soil and vegetation: A case study in the former lake Texcoco, Mexico. *Journal of Arid Environments*, 65(4), 644-667.
- Fourati, H. T., Bouaziz, M., Benzina, M., & Bouaziz, S. (2015). Modeling of soil salinity within a semi-arid region using spectral analysis. *Arabian Journal of Geosciences*, 8(12), 11175-11182.
- Makhdoum, M., Darvishsefat, A. S., Jafarzadeh, H., & Makhdoum, A. (2009). Assessment and planning of Environment with GIS. Tehran University Press.
- Mashimbye, Z. E. (2013). Remote sensing of salt-affected soils (Doctoral dissertation, Stellenbosch: Stellenbosch University).
- Medjani, F., Aissani, B., Labar, S., Djidel, M., Ducrot, D., Masse, A., & Hamilton, C. M. L. (2017). Identifying saline wetlands in an arid desert climate using Landsat remote sensing imagery. Application on Ouargla Basin, southeastern Algeria. *Arabian Journal of Geosciences*, 10(7), 176.
- Meng, L., Zhou, S., Zhang, H., & Bi, X. (2016). Estimating soil salinity in different landscapes of the Yellow River Delta through Landsat OLI/TIRS and ETM+ Data. *Journal of Coastal Conservation*, 20(4), 271-279.
- Metternicht, G. I., & Zinck, J. A. (2003). Remote sensing of soil salinity: potentials and constraints. *Remote sensing of Environment*, 85(1), 1-20.
- Morshed, M., Islam, T., & Jamil, R. (2016). Soil salinity detection from satellite image analysis: an integrated approach to salinity indices and field data. *Environmental Monitoring and Assessment*, 188(2), 119.
- Pattanaaik, S. K., Singh, O. P., Sahoo, R. N., & Singh, D. K. (2008). Irrigation induced soil salinity mapping through principal component analysis of remote sensing data. *Journal of Agricultural Physics*, 8, 29-36.
- Pohl, C., & Van Genderen, J. L. (2017). Remote sensing image fusion: A practical guide. CRC Press.
- Schofield, R., Thomas, D. S. G., & Kirkby, M. J. (2001). Causal processes of soil salinization in Tunisia, Spain and Hungary. *Land Degradation & Development*, 12(2), 163-181.
- Subramanian, P., Alamelu, N. R., & Aramudhan, M. (2006). Fusion of multispectral and panchromatic images and its quality assessment. *ARPN Journal of Engineering and Applied Sciences*, 9(10), 4126-4132.
- Tajgardan, T., Aioubi, Sh., Shataee, Sh., & Khormali, F. (2009). Soil salinity mapping using ETM+ remotely sensed data. *Journal of water and soil conservation*, 16(2), 1-18.
- Yu, H., Liu, M., Du, B., Wang, Z., Hu, L., & Zhang, B. (2018). Mapping Soil Salinity/Sodicity by using Landsat OLI Imagery and PLSR Algorithm over Semiarid West Jilin Province, China. *Sensors*, 18(4), 1048.